Pathogenicity of in-vivo generated intestinal Th17 lymphocytes is IFNγ dependent.

Giulia Nizzoli[1,2] *, Claudia Burrello[3,4] *, Fulvia Milena Cribiù[5], Giulia Lovati[4], Giulia Ercoli[5], Fiorenzo Botti[2,6], Elena Trombetta[7], Laura Porretti[7], Katia Todoerti[8], Antonino Neri[3,9], Maria Rita Giuffrè[2], Jens Geginat[10], Maurizio Vecchi[,1,11], Maria Rescigno[4], Moira Paroni[12] #, Flavio Caprioli[1,2] #, Federica Facciotti[4] #

1. Gastroenterology and Endoscopy Unit, Fondazione IRCCS Ca' Granda Ospedale Maggiore Policlinico, Milan, Italy;

2. Department of Pathophysiology and Transplantation, Università degli Studi di Milano, Milan, Italy;

3. Department of Oncology and Hemato-Oncology, University of Milan, Milan, Italy;

4. Department of Experimental Oncology, European Institute of Oncology, Milan, Italy;

5. Pathology Unit, Fondazione IRCCS Ca' Granda Ospedale Policlinico di Milano, Milan, Italy;

6. General and Emergency Surgery Unit, Fondazione IRCCS Ca' Granda Ospedale Maggiore Policlinico, Milan, Italy

7. Flow Cytometry Service, Clinical Chemistry and Microbiology Laboratory Fondazione IRCCS Ca' Granda Ospedale Maggiore Policlinico, Milan, Italy.

8. Laboratory of Pre-clinical and Translational Research, IRCCS-CROB, Referral Cancer Center of Basilicata, Rionero in Vulture, Italy;

9. Hematology Unit, Fondazione IRCCS Ca ' Granda, Ospedale Maggiore Policlinico, Milan, Italy;

10. INGM – National Institute of Molecular Genetics "Romeo ed Enrico Invernizzi" Milan,

Italy.

11 Department of Biomedical Sciences for Health, Università degli Studi di Milano, Milan, Italy

12. Department of Biosciences, Università degli Studi di Milano, Milan, Italy

Address for correspondence:

Flavio Caprioli, MD PhD

Department of Pathophysiology and Transplantation, University of Milan

Via Francesco Sforza, 35

20122 Milan, Italy

E-mail: flavio.caprioli@unimi.it

Telephone: +39 02 55033368   Fax: +39 02 55032140

* GN and CB; # FF, MP and FC equally contributed.

ABSTRACT

Background and aims. Th17 cells are crucially involved in the immunopathogenesis of inflammatory bowel diseases in humans. Nevertheless, pharmacological blockade of IL17A, the Th17 signature cytokine, yielded negative results in patients with Crohn's disease (CD), and attempts to elucidate the determinants of Th17 cells pathogenicity in the gut have so far proved unsuccessful. Here, we aimed to identify and functionally validate the pathogenic determinants of intestinal IL-17-producing T cells.

Methods *In-vivo* generated murine intestinal IL-17-producing T cells were adoptively transferred into immunodeficient $Rag1^{-/-}$ recipients to test their pathogenicity. Human IL-17-, IFNγ/ IL-17 and IFNγ- actively secreting T cell clones were generated from lamina propria lymphocytes of CD patients. The pathogenic activity of intestinal IL-17-producing T cells against the intestinal epithelium was evaluated.

Results. IL-17-producing cells with variable colitogenic activity can be generated *in-vivo* by different experimental colitis models. Pathogenicity of IL-17-secreting cells was directly dependent on their IFNγ secretion capacity, as demonstrated by the reduced colitogenic activity of IL-17-secreting cells isolated from IFNγ$^{-/-}$ mice. Moreover, IFNγ production is a distinguished attribute of CD-derived lamina propria Th17 cells. IFNγ secretion by CD-derived IL-17-producing intestinal clones is directly implicated in the epithelial barrier disruption through the modulation of tight junction proteins.

Conclusions. Intestinal Th17 cell pathogenicity is associated to IFNγ production, which directly affects intestinal permeability through the disruption of epithelial tight junctions.

INTRODUCTION

Crohn's disease (CD) and ulcerative colitis (UC), known as inflammatory bowel diseases (IBD), are chronic inflammatory disorders of the digestive tract [1]. Current theories suggest that IBD onset is secondary to an exaggerated reaction of gut-associated lymphoid tissue against the intestinal flora [2, 3] and that T helper (Th) cells, including Th17 cells, play a major role in orchestrating the inflammatory response [4].

IBD patients manifest increased amounts of intestinal Th17 cells [5], and a genome wide-association study identified genetic variants in the *IL23R* gene, encoding for the receptor of the Th-17 promoting cytokine IL-23, as independent protective factors for CD [6]. Nonetheless, a clinical trial aimed at blocking IL-17A in patients with luminal CD showed negative results [7]. The recent understanding that Th17 cells can be divided into at least two different subsets on the basis of cytokine profile and pathogenicity, probably explains these apparently conflicting results. Classical Th17 cells, induced in the presence of TGFβ1 and IL-6, have been found to display regulatory activities, owing to the co-production of IL-17 and IL-10 [8]. Alternative Th17 cells are instead characterized by the co-secretion of IL-17 and inflammatory cytokines, including IFNγ and GM-CSF, and can mediate pathogenic activities in experimental models of inflammation [9]. Several studies have corroborated the existence of a functional plasticity of Th17 cells towards the Th1 lineage, both in murine models and in human autoimmune diseases, including IBD [10]. The functional transition of T cells from classical Th17 to alternative Th1/17 lineage is mostly owed to T cell activation in the presence of interleukin-12 and interleukin-23, produced by antigen-presenting cells in response to bacteria-derived signals, and involved in the initiation of the Th1 transcriptional program [11].

At present, the factors associated with the pathogenicity of *in-vivo*-differentiated Th17

cells in the gut are yet to be fully elucidated. In this context, it has been suggested that IFNγ produced by *in-vitro*-differentiated Th17 cells might exert a pathogenic role in a murine model of intestinal inflammation [*12*]. On the other hand, recent evidence demonstrates that intestinal IL-17 expression acts in an IL-23-independent manner to maintain epithelial permeability through the regulation of tight junction expression [*13, 14*]. The inflammatory potential of Th17 cells in the gut has so far been studied either with *in-vitro* polarized cells [*12*], not fully recapitulating *in-vivo*-occurring Th17 cells from a functional standpoint [*8, 15-17*] or gut-derived Th17 cells induced *in vivo* by anti-CD3 antibody administration [*18*]. The relevant co-production of IL-10 by anti-CD3-induced intestinal Th17 cells [*19*], together with their reduced IFNγ expression, can however suggest that this model is not optimal to study Th17 pathogenic factors *in vivo*. Additionally, although the detrimental role of recombinant IFNγ on epithelial cell permeability has been established in *in vitro* models [*20*], how IFNγ acts in conferring colitogenic activity to *in-vivo*-differentiated cells in the gut is currently unknown.

In the present study, we adopted a translational approach aimed at elucidating the pathogenic factors of *in-vivo*-generated intestinal Th17 cells in experimental intestinal inflammation and human Th17 cells isolated from the intestinal mucosa of ileal Crohn's disease patients.

Matherial and Methods

Human Subjects. Peripheral blood and intestinal specimens were obtained from 27 patients with ileal or ileo-colonic Crohn's disease (CD) and 23 non-IBD controls (HD) at the IRCCS Ospedale Maggiore Policlinico (Milan, Italy). All the patients were categorized according to the Montreal classification. The clinical characteristics and

concomitant therapies of CD and HD patients are summarized in Table 1. The Institutional Review Board approved the study (permission ref. no. EA1/107/10) and informed consent was obtained from the patients. The study was performed in accordance with Declaration of Helsinki protocols.

Mice. C57Bl/6 mice were purchased from Charles River Laboratories. IL-17A-^{eGFP} (Singer), *IFN$\gamma^{-/-}$* and *Rag1$^{-/-}$* mice were purchased from Jackson Laboratories. IL-17A^{eGFP}x *IFN$\gamma^{-/-}$* and IL-17A^{eGFP}x *IFN$\gamma^{+/+}$* mice were generated at the IEO animal facility. Experimental mice (age and sex matched littermates, 8-10 weeks of age) were housed at the IEO animal facility in SPF conditions. Animal procedures were approved by Italy's Ministry of Health (Authorizations no. 27/13, 127/15, 913/16).

Murine and human cells isolation. Murine lamina propria mononuclear cells (LPMC) were isolated from colons and small intestines as in [*18*]. Mesenteric LN and spleens were smashed into 70-µm nylon strainers (BD) and eritrocytes lysed with RBC Lysis buffer (BD). Human LPMC were isolated as in [*51*].

In-vivo induction of murine Th17 cells. In the anti-CD3-induced colitis [*18*], intestinal Th17 cells were generated by injecting mice intraperitoneally (*i.p.)* with anti-CD3 antibodies (15 µg, clone 145-2C11) twice every other day. Mice were sacrificed 4 hours after the last injection.

In the adoptive transfer model [*21*], splenic CD4$^+$ T cells were enriched by magnetic separation (CD4 murine MicroBeads, clone L3T4, Miltenyi). CD4$^+$ T cells were sorted as

Lin-CD3$^+$CD4$^+$CD62L$^+$CD25$^-$ in a FACSAria cell sorter (BD) and 2.5x10^5 cells were injected *i.p.* in Rag1$^{-/-}$ mice. Donor splenocytes were isolated from IL-17A$^{eGFP/+}$, IL-17A $^{eGFP/+}$xIFN$\gamma^{-/-}$ or IL-17A $^{EGFP/+}$xIFN$\gamma^{+/+}$ mice.

Th17 in-vivo pathogenicity test by repetitive adoptive T cell transfer. The pathogenicity of *in-vivo*-generated murine Th17 cells was evaluated by repetitive adoptive transfers in Rag1-/- mice of IL-17A eGFP positive cells generated either by aCD3 injection (aCD3) or by adoptive transfer of splenic naïve T cells (AT1).

CD4+ IL-17A eGFP positive T cells (Lin-CD3+CD4+IL-17A eGFP+CD25-) generated in the aCD3 model were sorted on a FACSAria from the small intestines of injected mice, while those generated from the AT1 model were sorted from colons and mesenteric lymph nodes. 2.5X10^5 sorted cells were injected *i.p.* in a second Rag1-/- recipient (AT2). The gating strategy is illustrated in Supplementary Figure 1.

AT1, aCD3AT1 and AT2 mice were sacrificed 3 weeks following the adoptive transfer and the immune cell infiltrate as well as the histologic score were assessed. Small intestines and colons were removed and portioned to be fixed in 10% formalin or PLP buffer for histological analysis and immunofluorescence, snap-frozen for RNA extraction and processed for lamina propria mononuclear cells (LPMC) immuno-phenotyping. Before portioning, colon length was measured.

Histological analysis. For histological analysis tissue processing was performed with a LEICA PELORIS processor before paraffin embedding. Murine samples were embedded using an automated system (SAKURA Tissue-Tek). After hematoxylin and eosin

staining, snapshots of histology were taken using an Aperio CS2 microscope with a scanning resolution of 50,000 pixels per inch (0.5 μm per pixel with a 10x zoom and 2.5 μm per pixel when scanning at 4x). The scoring of disease activity was performed according to the criteria described in Supplementary Table 6.

Human intestinal T cell lines and clones generation. Human Th1, Th1/17 and Th17 clones were generated via cloning by limiting dilution according to the protocol described in [22] from sorted IL-17$^-$IFNγ^+, IL-17$^+$IFNγ^+ or IL-17+IFNγ^- CD4$^+$CD8$^-$CD25$^-$ T cells.

For the isolation of cytokine-producing lymphocytes, freshly isolated total LPMC were *in-vitro* stimulated for 3 hours with PMA/Ionomycin (1 μg/ml), and CD4$^+$ IL-17$^-$IFNγ^+ (Th1), IL-17$^+$IFNγ^+ (Th1-17) or IL-17+IFNγ^- (Th17) cells were sorted by flow cytometry with IL-17A and IFNγ Secretion assays (Miltenyi).

Th1, Th1-17 and Th17 cells were cloned by limiting dilution and re-stimulated with irradiated feeder cells, PHA (1 μg/ml, Sigma) and hIL-2 (100 U/ml, Proleukin) every 21 days.

Flow cytometry. Murine and human cells were stained with combinations of directly conjugated antibodies as specified in Supplementary Table 1C, all sourced from BD, eBioscience or Biolegend. The gating strategy to identify murine T cells included the exclusion of CD11b+, CD19+ and CD11c+ cells (defined as "lineage").

The proliferation of colonic T cells was assessed by Ki-67 staining (Biolegend) according to the manufacturer's protocol. The apoptosis of epithelial cells was assessed by Annexin V staining (Biolegend).

Intracellular cytokines were detected after stimulation of murine and human cells for 3 hours with 0.1µM PMA and 1µg/ml Ionomycin (Sigma-Aldrich). 10µg/ml Brefeldin A (Sigma) was added for the last hour of stimulation. Cells were fixed and permeabilized with Cytofix/Cytoperm (BD) before the addition of the antibodies detecting the cytokine released.

Multiplexing analysis of cytokines in supernatants collected after T cell clones stimulation with PMA/Ionomycin was performed with a CBA assay, according to manufacturer's protocol (BD).

Samples were analyzed by a FACSCanto flow cytometer (BD), gated to exclude non-viable cells on the basis of light scatter. Data were analyzed using FlowJo software (Tristar).

Immunofluorescence. Intestinal samples were fixed overnight in paraformaldehyde (PFA), L-Lysine pH 7.4 and NaIO4 (PLP buffer). They were then washed, dehydrated in 20% sucrose for at least 4 hours and included in OCT (Sakura). 10µm-thick sections were re-hydrated with a 0.1M Tris HCl ph7.4 buffer and blocked with 0.3% Triton X-100, 2% FBS 0.1M Tris-HCl buffer. For ZO-1 staining, the slides were incubated with the primary antibody (anti-ZO-1 FITC, 1:100) for 2 hours. For CCL20 staining the slides were incubated with the primary antibody (anti CCL20, 1:100) overnight and then with AF647 secondary antibody for 2 hours. Nuclei were counter-stained with DAPI (1:30.000; Roche) and mounted with Vectashield (Vector Laboratories).

Lab-Tek culture chamber slides (Sigma) with monolayers of Caco-2 cells were fixed with 4% PFA before blocking with 2% FBS-containing Tris-HCl buffer and staining of fluorocrome-conjugated anti-ZO-1 antibodies (1:100). The slides were mounted with a

fluorescent mounting medium (Dako Cytomation) and analyzed by using an inverted confocal laser scanning microscope (Leica). Digital images were taken and processed using Fiji software.

RNA isolation, cDNA synthesis, quantitative PCR and gene expression. Total RNA was extracted from mouse intestinal tissues using TRIZOL and Quick-RNA MiniPrep (Zymo Research) according to the manufacturer's instructions, and from Caco-2 cells using RNeasy Micro Plus kit, Qiagen. cDNAs were retro-transcribed with EasyScript Plus Reverse Transcriptase kit (abm Inc.) and amplified with in-vitro DNA Amplification Kit (abm Inc.). Gene expression levels were evaluated by qPCR using SYBR Green Master Mix (Applied Biosystems) and normalized to murine Rpl32 or human GAPDH gene expression. Primer sequences used for qPCR analysis are available in Supplementary Table 1a. An heat map was generated on the average of the standardized expression value (Z-score) of selected genes by Expression Heatmaps function on Heatmapper server (http: http://www1.heatmapper.ca/).

For global gene expression profiling analysis, total RNA samples from healthy control and Crohn's disease patients were processed according to the manufacturer's protocol, by using GeneChip Human Gene 1.0 ST array (Affymetrix, Santa Clara, CA). The raw intensity expression values were processed by Robust Multi-array Average procedure [49] , with the re-annotated Chip Definition Files from BrainArray libraries version 20.0.0 [50], available at http://brainarray.mbni.med.umich.edu. In order to find the differentially expressed genes between Crohn's disease patients and control samples, global gene expression analysis was perfomed on two separate datasets. The ratio of the difference between the expression levels of the two experiments on the mean value of the same

two variables was computed. Those genes exceeding the mean plus 3 standard deviations of all the ratio values were selected as the most significantly differentially expressed between the two conditions. Functional annotation clustering was performed on Gene Ontology (GO) terms using the default conditions, by means of the Database for Annotation, Visualization and Integrated Discovery (DAVID) Tool 6.8 (https://david.ncifcrf.gov/). Annotation clusters with an Enrichment Score (ES) >1.3 were chosen and representative GO terms were reported for each significant cluster.

In-vivo intestinal permeability measurement. The permeability of the intestinal epithelial/endothelial barrier *in vivo* was measured by analysis of the LPS concentration in the blood serum of mice with LAL Chromogenic Endotoxin Quantitation Kit (Pierce, Thermo Fisher) according to manufacturer's protocol.

Measurement of trans-epithelial electrical resistance (TEER). The Caco-2 cells were sourced from the American Type Culture Collection (ATCC) and cultured in DMEM supplemented with 20% FCS, 2MM L-glutamine, 1mM sodium pyruvate, 0.1 mM non-essential amino acids (NEAA) and penicillin/streptomycin. The cells were split three times a week. For TEER measurement the cells at passage 10-30 were plated at 15×10^3 cells/well on polyester permeable Transwell-clear inserts (6.5-mm diameter, 0.4-mm pore size, Corning®) and grown for 5–7 days, until ΔTEER >300 Ω*cm2 (Millicell-ERS Volt-Ohm Meter Millipore, Bedford, MA).

The supernatants collected from intestinal CD4+ T cell clones, stimulated for 3 hours with PMA/ionomycin in Caco-2 medium, in the presence or absence of neutralizing Ab (anti- human -IFNγ, -IL-17A, -TNF, eBioscience 10 µg/ml, 20 µg/ml for anti-IFNγ) were

applied in the lower transwell chamber. Human recombinant cytokines (rIL-1β, and rTNF, 10µg/ml, Miltenyi) were used as positive controls.

Measurements were carried out every 30 minutes in the first 2 hours, then at 24 and 48 hours after stimulation. The ohmic resistance of a blank (culture insert without cells) was measured in parallel. To obtain the sample resistance, the blank value was subtracted from the total resistance of the sample. The final unit area resistance (Ω*cm2) was calculated by multiplying the sample resistance by the effective area of the membrane. For comparison among treatments with different clones, TEER was normalized to the supernatant of each unstimulated clone.

Tight junction expression on intestinal cell monolayers. Caco-2 cells were seeded on 8-well Lab-Tek culture slides (Sigma), at a density of 104 cells/well in complete DMEM medium. Once 90% confluence was reached, the medium was replaced by 400 ul of supernatant derived from stimulated human T-cell clones; as negative controls, the medium alone or the supernatant of unstimulated clones were used. rIL-1b and rTNF (10 ug/ml, Miltenyi) were used as positive controls. Caco-2 cells were stimulated for 16 hours and then fixed and the tight junction expression was evaluated by IF microscopy (Zonulin-1) or by qPCR analysis.

Statistics. Statistical significance was calculated by a two-tailed unpaired Mann-Whitney test without assuming a Gaussian distribution. P <0.05 (*), P <0.01 (**) P <0.001 (***) were regarded as statistically significant. Outliers were detected with Grubb's test.

RESULTS

Intestinal IL-17-producing cells with different colitogenic potential can be generated in vivo.

Intestinal Th17 cells were generated *in vivo* through different experimental protocols (Fig 1A, 1B) and IL-17-producing cells were tracked by the use of IL-17$^{eGFP/+}$ reporter mice [19]. The intraperitoneal injection of the anti-CD3 antibody 2C11 into IL-17$^{eGFP/+}$ mice (aCD3, Fig. 1A, left panel) induced the differentiation of intestinal Th17 cells co-producing IL-10 and IL-22, but not IFNγ (Fig. 1C). On the contrary, the adoptive transfer of naïve T cells into Rag1$^{-/-}$ recipients [21] (AT1, Fig. 1B, left panel) induced Th17 cells that were co-secreting IFNγ but very little IL-10 and IL-22 (Fig. 1C, D and Supplementary Figure 2A).

The colitogenic potential of intestinal Th17 cells differentiated *in-vivo* by these two protocols was evaluated by adoptive transfer of the sorted intestinal IL-17^{eGFP} cells from aCD3 or AT1 mice into a second immunodeficient Rag1$^{-/-}$ host (aCD3-AT2, Fig. 1A; and AT2, Fig. 1B right panels). Intestinal IL-17^{eGFP} cells originated from aCD3 or AT1 mice expressed similar levels of CD69 and α4β7, confirming similar activation status and intestine-homing ability (not shown). Three weeks after the adoptive transfer of IL-17-producing cells, the histological examination of aCD3-AT2 mice highlighted a milder intestinal inflammation as compared to AT2 mice (Fig. 1E–1F) and a lower colonic expression of Th1-associated genes including *cxcr3* (Fig. 1G) and *tnf* (Fig. 1H). Noteworthy, the AT2 mice expressed increased colonic levels of *ccl20*, a chemokine promoting CCR6$^+$Th17 cells recruitment in the mucosa [19] (Fig. 1G).

Colonic CD4$^+$ T cells isolated from AT2 mice held a sustained IFNγ-secreting capacity (Fig. 1I,J and Supplementary Figure 2B), an activated CD69$^+$ phenotype, and expressed

high levels of the gut-homing integrin $\alpha4\beta7$ (Fig. 1K) three weeks post transfer. On the contrary, CD4$^+$ T cells isolated from aCD3-AT2 mice secreted more IL-10 in both the colon and mLN and expressed lower levels of CD69 and $\alpha4\beta7$ (Fig. 1I-K). To note, colonic IL-17$^+$ cells of AT2 mice were also robustly proliferating, as indicated by the Ki-67 expression (Fig. 1L) and the increased absolute numbers (data not shown).

Taken together, these data support the possibility to induce *in-vivo* intestinal Th17 cells exhibiting different pathogenic potentials associated with a skewed cytokine co-expression profile.

IFNγ confers pathogenic activity to intestinal IL-17-producing T cells.

To evaluate if IFNγ produced by *in-vivo* generated intestinal IL-17$^+$ cells contributed to their colitogenic activity, we firstly crossed IL-17A^{eGFP} mice with IFNγ $^{-/-}$ mice (Suppl. Fig. 3). Next, IFNγ-sufficient or -deficient Th17 cells were generated *in vivo* by adoptively transferring naïve T cells isolated from IL-17^{eGFP}IFN$\gamma^{+/+}$ or IL-17^{eGFP}IFNγ $^{-/-}$ mice (AT1, Fig. 2A, left panel). Of note, IFNγ-sufficient or -deficient Th17 cells were characterized by a similar phenotype (supplementary Figure 4A). Finally, the pathogenicity of IFNγ-sufficient or deficient Th17 cells was tested by transferring colonic IL-17^{eGFP} positive cells into a second immunodeficient host (IFN$\gamma^{+/+}$AT2 and IFN$\gamma^{-/-}$AT2, Fig. 2A right panel).

The transfer of *in-vivo*-differentiated colonic IFNγ-deficient-Th17 cells induced a milder form of colitis than that induced by IFNγ-sufficient-Th17 cells, as shown by histological evaluation (Fig. 2B) and colon length measurement (Fig. 2C). Colonic CD4+ T cells isolated from IFN$\gamma^{-/-}$AT2 mice showed a reduced proliferative capacity (Supplementary figure 4B) and a skew towards IL-10 production, to suggest a negative control of IFNγ over IL-10 production in Th17 cells (Fig. 2D). The latter phenomenon may also

contribute to the reduction of T- cell-derived IL-17 and IL22 in IFNγ$^{-/-}$AT2 mice, confirming a suppressive role of IL-10 over Th17 cytokine production [22].

The transfer of pathogenic IFNγ-sufficient Th17 cells led to a significant increase in the colonic expression of ccl20, at RNA (Fig. 2E) and protein level (Fig. 2F), which was not observed in recipients of IFNγ-deficient-Th17 cells, No significant differences between the recipients of IFNγ-deficient or -sufficient Th17 cells were observed with regard to the colonic expression of other chemokines or inflammatory genes (Fig. 2F) with the notable exception of *tnf*, which was reduced, albeit not significantly, in IFNγ$^{-/}$AT2 mice (Fig. 2G).

In order to assess whether Th17-derived IFNγ exerted any influence over intestinal permeability, the circulating levels of lipopolysaccharide (LPS), a marker of bacterial translocation and an indirect marker of epithelial barrier integrity [23], were measured in recipients of intestinal Th17 cells. Reduced LPS levels were found in mice receiving IFNγ-deficient with respect to IFNγ-sufficient Th17 cells (Fig. 2H). This was associated with enhanced protein levels of the intestinal tight junction protein zo-1 in the intestinal epithelium (Fig. 2I).

Taken together, these results suggest that IFNγ contributes to the pathogenic activity of *in-vivo*-generated intestinal Th17 cells by exerting a direct effect over the epithelial barrier, and by inhibiting IL-10 intestinal expression.

Characterization of IL-17-producing cells from CD patients.

We next evaluated whether the functional phenotype of murine intestinal pathogenic Th17 cells would be retained in human Crohn's disease. The cytokine profile of the lamina propria CD4$^+$ Th cells of CD patients and uninflamed controls (*i.e*, patients undergoing intestinal resections for cancer or IBD-unrelated pathologies) (Table 1) was analyzed *ex vivo* by cytofluorimetry (Fig. 3A–3D and Suppl. Fig. 5A). To minimize

biological variability, the analysis was exclusively focused on surgical terminal ileal specimens. As previously reported [*10*], a significant co-expression of IFNγ and TNF was observed in the IL-17-producing cells isolated from the CD patients, but not from the uninflamed controls (Fig. 3A and 3C). In contrast, almost no IL-17$^+$IL10$^+$ CD4$^+$ cells were found in CD and HD LPMC (Fig. 3B and 3D), while an increased proportion, albeit not statistically significant, of IL-17$^+$IL22$^+$ was observed in CD mucosa.

Next, we evaluated if a gene expression signature for CD-derived lamina propria Th17 cells existed. Actively IL-17-secreting ileal CD4$^+$ Th cells were *ex-vivo* sorted from CD and HD LPMC (Fig. 3E and Suppl. Fig. 5B). As expected, only IL-17$^+$ CD4$^+$ sorted Th cells, but not IL-17$^-$ cells, expressed the gene transcript for IL-17 (Fig. 3F). Of note, the expression of the gene encoding for *ifng* was strongly associated to CD-derived IL-17$^+$ CD4$^+$ T cells (Fig. 3G), while the gene encoding for *TNF* was mostly associated to IL-17$^-$ T cells. Next, a global transcriptional profiling of the sorted lamina propria IL-17-producing CD4$^+$ T cells from CD and healthy mucosa was performed by microarray analysis on ultra-high quality RNA (Fig. 3H–3J). Functional annotation clustering was performed on the 211 differentially expressed genes (149 upregulated, 62 downregulated) in CD-derived IL-17$^+$ cells as compared to those from healthy mucosa. A significant enrichment in specific functional categories, such as responses to microbial stimuli, activation, co-stimulation and cytokine-mediated T cell signaling was evidenced (Fig. 3I). Fold changes in expression levels between CD and healthy samples were depicted for genes involved in transcription regulation, acting as cell surface molecules or chemokines and cytokines (Fig. 3J). Interestingly, Th17 from uninflamed ileum expressed increased levels of IL-9, which is a cytokine associated with 'classical' Th17 cell gene signature [*9, 24*].

Taken together, these data indicate that IL-17-secreting CD4$^+$ T cells from CD patients

express distinct cytokine and molecular profiles and confirm that IFNγ might be a distinguished attribute for human CD-derived Th17 cells [10].

Intestinal Th1-17 clones exert distinctive effects on epithelial cells.

We next investigated whether human Th17 cells isolated from the intestinal mucosa of active CD patients conveyed similar IFNγ-mediated pathogenic effects towards the intestinal epithelium integrity. To this end, CD4$^+$ T cells were isolated from LPMC in 6 active treatment-naïve ileal CD patients. By taking advantage of a double IFNγ/IL-17-secretion assay (Fig. 4A), lamina propria IL-17-, IFNγ- or both IL-17/IFNγ - actively secreting CD4$^+$T cells were *ex vivo* sorted and subsequently cloned by limiting dilution [25] in order to generate respectively Th17, Th1 and Th1-17 stable clones (Fig. 4B, 4C). To note, the total number of clones that could be generated from each patient was variable and partly reflected the inflammatory status of the mucosa and the disease course (Fig. 4B). To prevent possible artifacts linked to Th17 cones plasticity [26], the cytokine profile of Th1, Th1-17 and Th17 CD4$^+$ T cell clones was re-evaluated by flow cytometry before each functional assay. In addition, functional assays were performed with at least 3 to 5 independent clones for each subset.

Soluble mediators, including cytokines, produced by the immune cells during intestinal inflammation can directly act on the mucosal epithelial barrier [27]. To evaluate the contribution of Th cell-derived soluble factors to the intestinal epithelial damage, the supernatants of polyclonally activated CD-derived Th clones were applied on Caco-2 colon epithelial monolayers. Multiplexing analysis demonstrated a higher amount of IFNγ, TNF and GM-CSF in Th1 and Th1/17-derived supernatants, which were not detected in Th17-derived supernatants (Fig. 4D). The supernatants of activated Th1 or

Th1-17 clones, but not of Th17 clones, affected the integrity of the epithelial layer, as documented by a significant reduction of the transepithelial electrical resistance (TEER, Fig. 4E). The pathogenic effects of Th1 and Th1-17-derived supernatants were associated with the disruption of the monolayer architecture, as shown by tight junction protein ZO-1 immunofluorescence staining (Fig. 4F). Annexin V staining and early apoptotic gene expression analysis in epithelial cells excluded any contribution of T cell-mediated apoptosis in modulating epithelial cell permeability (Suppl. Fig.6). Importantly, *ccl20* mRNA induction in Caco-2 cells was exclusively observed following stimulation by Th1/17 supernatants (Fig. 4G).

These data confirm that IL-17-producing cells isolated from CD patients contain an elevated proportion of Th1/17 cells that exhibit pathogenic activity against the integrity of the intestinal epithelial barrier.

IFNγ produced by Th1-17 clones is responsible for pathogenicity against intestinal epithelial cells.

To link the IFNγ produced by Th17 cells to the observed effects on epithelial cells permeability, supernatants of polyclonally stimulated human Th1, Th1-17 and Th17 clones were applied *in vitro* to Caco-2 monolayers in the presence of IFNγ neutralization (Fig. 5A). TEER measurement (Fig. 5A) demonstrated that IFNγ neutralization suppressed the effect of the Th1 and Th1-17 clone supernatants, but not that of pure Th17 clones, over epithelial permeability. Additionally, IFNγ neutralization partially restored the RNA expression levels of several junctional proteins (Fig. 5B), More importantly, it prevented architectural disruption in Caco-2 monolayers exposed to Th1-17 clones supernatants (Fig. 5C).

In conclusion, these data confirm that IFNγ secreted by IL-17-producing T cells during intestinal inflammation has a direct pathogenic effect on the intestinal epithelium and its blockade reduces intestinal permeability by modulating tight junction expression.

DISCUSSION

The negative outcomes of IL-17A neutralization in CD patients [7] led to a progressive reconsideration of the role of Th17 cells and Th17-derived cytokines in the modulation of intestinal inflammation and in IBD pathogenesis. The results from the present study demonstrate that *in-vivo*-generated intestinal Th17 cells exert a pathogenic activity in the gut, which is linked to their transition towards Th1/17 cells, and is mostly mediated by IFNγ activity towards the epithelial barrier.

The plasticity of mature Th17 lymphocytes towards IFNγ-production in response to inflammatory milieu is an established concept. IL-23 signalling, in particular, is a key factor mediating Th17 to Th1 transition. Similarly, the *in-vitro* exposure of Th17 precursors to IL-23 results in the progressive extinction of IL-17A and emergence of IFNγ-producing cells [24]. Th17-Th1 transition has been also causally related to the emergence of intestinal inflammation, as the transfer of *in-vitro*-generated Th17 cells gives rise to IFNγ-producing cells in the gut, and induces colitis that is partially reversed by IL-23 neutralization [24, 28]. Gut-derived Th1, Th17 and Th1/17 cells exert a similar colitogenic activity, upon the switch towards Th1-like cells and IFNγ production [29].

In our study, Th17 cells, differentiated *in vivo* in two distinct colitis models, induced some degree of intestinal inflammation. Nevertheless, the transfer of intestinal IL-17+ cells, harvested from the adoptive transfer model, induced a higher colitis score, which was associated with a two-fold increase in T-cell IFNγ secretion. On the contrary, aCD3-derived Th17 cells showed persistent IL-10 secretion, thus confirming the previously

reported ineffectiveness of IL-17$^+$IL-10$^+$ cells in sustaining pathological inflammation [8]. As Th17 cells express a functional IL-10 receptor [18], one can speculate that Th17-derived IL-10 potentially contributes to the restraining of Th17-mediated inflammation in the colon. Moreover, IL-10 neutralization was required for the efficient transition of Th17 cells towards IFNγ$^+$ production in a T cell transfer colitis model [29].

The determinants of Th17-to-Th1 transition in the gut are still to be clarified, but current evidence suggests that intestinal flora possibly plays a relevant role [11]. Morrison *et al.* have demonstrated that *Helicobacter hepaticus* infection induces intestinal Th17 cells that progressively extinguish IL-17A secretion and turn IFNγ on [29]. CD-derived LPMCs secrete IFNγ following their exposure to commensal bacteria, in a process partly mediated by IL-23 production from intestinal antigen-presenting cells [30, 31]. Finally, gut-derived Th17 cells are characterized by a T-cell antigen receptor (TCR) repertoire, which is partly skewed towards the recognition of Segmented Filamentous Bacteria (SFB) and contributes to their pathogenic functions [32].

A strong association between T cell-derived IFNγ and experimental intestinal inflammation has been long known. IFNγ neutralization inhibits colitis development in a CD45RB^{hi} T cell transfer model [21]. Similarly, T cells derived from IFNγ- [33] Tbet- [34] or STAT4- [35] deficient mice fail to induce intestinal inflammation upon transfer. Recently, IFNγ production by *in-vitro*-differentiated Th17 cells has shown to contribute to their pathogenic activity [12]. However, *in-vitro*-differentiated Th17 cells do not fully recapitulate those arising *in vivo* under homeostatic or inflammatory conditions [12], [8, 15–17].

Live murine cytokine-secreting cells can be easily tracked thanks to the availability of different reporter mice. To isolate live IL-17 and IFNγ-secreting cells from human

specimens, instead, we took advantage of a cytokine secretion assay coupled with cell sorting, followed either by RNA extraction or by single cell cloning. To our knowledge, this is the first time that this technique has been applied to the functional study of human intestinal T cells. This approach has proved to be technically challenging, given the reduced number of cells isolated from human intestinal specimens, their intrinsic fragility, and the complex steps required from isolation, stimulation, sorting and cloning. Nonetheless, this technique has proved successful and allowed us to perform functional assays, and gene expression profiles, with unmanipulated CD-derived pathogenic CD4+ human intestinal T cell subsets (Th17, Th1/17 and Th1), defined by their cytokine profile rather than by surface markers expression [*36-38*].

Increased epithelial barrier permeability and bacterial translocation are considered crucial events in IBD development [*3*] and mucosal T cells have shown to contribute in multiple ways [*39*]. Intestinal epithelial cells express IFNγR [*40*] and recombinant IFNγ applied to intestinal epithelial cell lines decreases their transepithelial resistence [*41*], an effect that is prevented by an anti-IFNγR antibody [*42*]. Here, we observed that pro-inflammatory cytokines secreted by Th1 and Th1/17-intestinal clones from IBD patients are directly responsible for the increase in epithelial barrier permeability. Th1 and Th1/17-derived IFNγ increased epithelial cell permeability by acting on the junctional proteins, particularly zonulin-1 (ZO-1): this confirms previous data obtained with recombinant IFNγ [*41*]. Although IFNγ can induce apoptosis in many cell lines, alone or with IL-1b and TNF [*44*], we could not observe IFNγ-induced apoptosis in epithelial cells. However, a direct association between IFNγ-dependent apoptosis and increased epithelial permeability has not been reported [*41, 42*].

The evidence that we have provided in this work, strongly suggests the direct

contribution of IFNγ as produced by Th17 cells in sustaining an inflammatory loop in IBD patients, which originates from an increase in EC permeability and possibly facilitates bacterial translocation to the lamina propria. In murine models, repetitive enteric stress induction elevates colonic IFNγ, which increases paracellular permeability and commensal bacterial translocation, not observed in IFNγ-deficient [*45*] or in anti-IFNγ treated mice [*46*]. To note, IFNγ promotes also the intracellular epithelial internalization of bacteria [*47, 48*].

Thus, our work provides the first direct association between the role of Th17-Th1 plasticity and Th17 IFNγ production in sustaining intestinal permeability and in mediating the Th17 cells pathogenic functions during experimental intestinal inflammation and human CD. These findings potentially lead to novel therapeutic opportunities to be aimed at blocking specific Th1-associated functions in Th17 cells, leaving unaltered those unrelated to intestinal inflammation that can instead contribute to regulatory functions.

ACKNOWLEDGMENTS

AUTHOR CONTRIBUTIONS

NG, CB performed experiments, analysed and interpreted data; GL and MRG performed the experiments of the revision; FMC and GE performed and interpreted histological analyses; FB recruited patients; ET, LP FACS-sorted cells; KT, AN performed and analysed global gene expression profiling; JG, MV and MR contributed to

interpretation of the data and gave important intellectual contributions and revised

the manuscript; MP, FC, FF designed and conceived the study; FC and FF supervised

the study and wrote the manuscript.

DISCLOSURE

The Authors have declared that no conflict of interests exists.

REFERENCES

1. M. Z. Cader, A. Kaser, Recent advances in inflammatory bowel disease: mucosal immune cells in intestinal inflammation. *Gut* **62**, 1653-1664 (2013).

2. Y. Belkaid, T. W. Hand, Role of the microbiota in immunity and inflammation. *Cell* **157**, 121-141 (2014).

3. A. Kaser, S. Zeissig, R. S. Blumberg, Inflammatory bowel disease. *Annu Rev Immunol* **28**, 573-621 (2010).

4. F. Caprioli, F. Pallone, G. Monteleone, Th17 immune response in IBD: A new pathogenic mechanism. *Journal of Crohn's & colitis* **2**, 291-295 (2008).

5. S. Fujino *et al.*, Increased expression of interleukin 17 in inflammatory bowel disease. *Gut* **52**, 65-70 (2003).

6. R. H. Duerr *et al.*, A genome-wide association study identifies IL23R as an inflammatory bowel disease gene. *Science* **314**, 1461-1463 (2006).

7. W. Hueber *et al.*, Secukinumab, a human anti-IL-17A monoclonal antibody, for moderate to severe Crohn's disease: unexpected results of a randomised, double-blind placebo-controlled trial. *Gut* **61**, 1693-1700 (2012).

8. M. J. McGeachy *et al.*, TGF-beta and IL-6 drive the production of IL-17 and IL-10 by T cells and restrain T(H)-17 cell-mediated pathology. *Nature immunology* **8**, 1390-1397 (2007).

9. A. Peters, Y. Lee, V. K. Kuchroo, The many faces of Th17 cells. *Curr Opin Immunol* **23**, 702-706 (2011).

10. F. Annunziato *et al.*, Phenotypic and functional features of human Th17 cells. *The Journal of experimental medicine* **204**, 1849-1861 (2007).

11. J. H. Chewning, C. T. Weaver, Development and survival of Th17 cells within the intestines: the influence of microbiome- and diet-derived signals. *J Immunol* **193**, 4769-4777 (2014).

12. S. N. Harbour, C. L. Maynard, C. L. Zindl, T. R. Schoeb, C. T. Weaver, Th17 cells give rise to Th1 cells that are required for the pathogenesis of colitis. *Proceedings of the National Academy of Sciences of the United States of America* **112**, 7061-7066 (2015).

13. J.S. Lee, *et al.* Interleukin-23-independent IL-17 production regulates intestinal epithelial permeability. *Immunity* **43,** 727-38 (2015).

14. J.R. Maxwell, *et al.* Differential roles for interleukin-23 and interleukin-17 in intestinal immunoregulation. *Immunity* **43,** 739-50 (2015).

15.   M. Janke *et al.*, In-vitro-induced Th17 cells fail to induce inflammation in vivo and show an impaired migration into inflamed sites. *European journal of immunology* **40**, 1089-1098 (2010).

16.   M. H. Lexberg *et al.*, Th memory for interleukin-17 expression is stable in vivo. *European journal of immunology* **38**, 2654-2664 (2008).

17.   K. Ghoreschi *et al.*, Generation of pathogenic T(H)17 cells in the absence of TGF-beta signalling. *Nature* **467**, 967-971 (2010).

18.   S. Huber *et al.*, Th17 cells express interleukin-10 receptor and are controlled by Foxp3(-) and Foxp3+ regulatory CD4+ T cells in an interleukin-10-dependent manner. *Immunity* **34**, 554-565 (2011).

19.   E. Esplugues *et al.*, Control of TH17 cells occurs in the small intestine. *Nature* **475**, 514-518 (2011).

20.   K. Juuti-Uusitalu *et al,* Differential effects of TNF (TNFSF2) and IFN-g on intestinal epithelial cell morphogenesis and barrier functions in three-dimensional culture. *Plos One* **6,** e22967 (2011)

21.   F. Powrie *et al.*, Inhibition of Th1 responses prevents inflammatory bowel disease in SCID mice reconstituted with CD45RBhi CD4+ T cells. *Immunity* **1**, 553-562 (1994).

22.   Y. Gu *et al.*, Interleukin 10 suppresses Th17 cytokines secreted by macrophages and T cells. *European journal of immunology* **38**, 1807-1813 (2008).

23.   O. Pastor Rojo *et al.*, Serum lipopolysaccharide-binding protein in endotoxemic patients with inflammatory bowel disease. *Inflammatory bowel diseases* **13**, 269-277 (2007).

24.   Y. K. Lee *et al.*, Late developmental plasticity in the T helper 17 lineage. *Immunity* **30**, 92-107 (2009).

25.   G. D. Libero. G. D. Libero, Ed., T cell protocols (Springer Editor, 2009).

26.   F. Annunziato, S. Romagnani, The transient nature of the Th17 phenotype. *European journal of immunology* **40**, 3312-3316 (2010).

27.   N. Wittkopf, M. F. Neurath, C. Becker, Immune-epithelial crosstalk at the intestinal surface. *Journal of gastroenterology* **49**, 375-387 (2014).

28.   P. P. Ahern *et al.*, Interleukin-23 drives intestinal inflammation through direct activity on T cells. *Immunity* **33**, 279-288 (2010).

29.   P. J. Morrison *et al.*, Th17-cell plasticity in Helicobacter hepaticus-induced intestinal inflammation. *Mucosal immunology* **6**, 1143-1156 (2013).

30. N. Kamada *et al.*, Unique CD14 intestinal macrophages contribute to the pathogenesis of Crohn disease via IL-23/IFN-gamma axis. *The Journal of clinical investigation* **118**, 2269-2280 (2008).

31. M. A. Kinnebrew *et al.*, Interleukin 23 production by intestinal CD103(+)CD11b(+) dendritic cells in response to bacterial flagellin enhances mucosal innate immune defense. *Immunity* **36**, 276-287 (2012).

32. Y. Yang *et al.*, Focused specificity of intestinal TH17 cells towards commensal bacterial antigens. *Nature* **510**, 152-156 (2014).

33. H. Ito, C. G. Fathman, CD45RBhigh CD4+ T cells from IFN-gamma knockout mice do not induce wasting disease. *Journal of autoimmunity* **10**, 455-459 (1997).

34. M. F. Neurath *et al.*, The transcription factor T-bet regulates mucosal T cell activation in experimental colitis and Crohn's disease. *The Journal of experimental medicine* **195**, 1129-1143 (2002).

35. S. J. Simpson *et al.*, T cell-mediated pathology in two models of experimental colitis depends predominantly on the interleukin 12/Signal transducer and activator of transcription (Stat)-4 pathway, but is not conditional on interferon gamma expression by T cells. *The Journal of experimental medicine* **187**, 1225-1234 (1998).

36. C. E. Zielinski *et al.*, Pathogen-induced human TH17 cells produce IFN-gamma or IL-10 and are regulated by IL-1beta. *Nature* **484**, 514-518 (2012).

37. J. Geginat *et al.*, The CD4-centered universe of human T cell subsets. *Semin Immunol* **25**, 252-262 (2013).

38. M. Paroni *et al.*, Recognition of viral and self-antigens by TH1 and TH1/TH17 central memory cells in patients with multiple sclerosis reveals distinct roles in immune surveillance and relapses. *J Allergy Clin Immunol*, (2017).

39. T. T. MacDonald, J. Spencer, Evidence that activated mucosal T cells play a role in the pathogenesis of enteropathy in human small intestine. *The Journal of experimental medicine* **167**, 1341-1349 (1988).

40. G. Valente *et al.*, Distribution of interferon-gamma receptor in human tissues. *European journal of immunology* **22**, 2403-2412 (1992).

41. J. L. Madara, J. Stafford, Interferon-gamma directly affects barrier function of cultured intestinal epithelial monolayers. *The Journal of clinical investigation* **83**, 724-727 (1989).

42. R. B. Adams, S. M. Planchon, J. K. Roche, IFN-gamma modulation of epithelial barrier function. Time course, reversibility, and site of cytokine binding. *J Immunol* **150**, 2356-2363 (1993).

43.   A. Youakim, M. Ahdieh, Interferon-gamma decreases barrier function in T84 cells by reducing ZO-1 levels and disrupting apical actin. *The American journal of physiology* **276**, G1279-1288 (1999).

44.   E. Vercammen *et al.*, Prolonged exposure to IL-1beta and IFNgamma induces necrosis of L929 tumor cells via a p38MAPK/NF-kappaB/NO-dependent mechanism. *Oncogene* **27**, 3780-3788 (2008).

45.   L. Ferrier *et al.*, Stress-induced disruption of colonic epithelial barrier: role of interferon-gamma and myosin light chain kinase in mice. *Gastroenterology* **125**, 795-804 (2003).

46.   M. D. Luyer *et al.*, Exposure to bacterial DNA before hemorrhagic shock strongly aggravates systemic inflammation and gut barrier loss via an IFN-gamma-dependent route. *Ann Surg* **245**, 795-802 (2007).

47.   E. Clark, C. Hoare, J. Tanianis-Hughes, G. L. Carlson, G. Warhurst, Interferon gamma induces translocation of commensal Escherichia coli across gut epithelial cells via a lipid raft-mediated process. *Gastroenterology* **128**, 1258-1267 (2005).

48.   D. M. McKay *et al.*, Phosphatidylinositol 3'-kinase is a critical mediator of interferon-gamma-induced increases in enteric epithelial permeability. *J Pharmacol Exp Ther* **320**, 1013-1022 (2007).

49.   R. A. Irizarry *et al.*, Exploration, normalization, and summaries of high density oligonucleotide array probe level data. *Biostatistics* **4**, 249-264 (2003).

50.   M. Dai *et al.*, Evolving gene/transcript definitions significantly alter the interpretation of GeneChip data. *Nucleic Acids Res* **33**, e175 (2005).

51.   F. Caprioli *et al.*, Autocrine regulation of IL-21 production in human T lymphocytes. *J Immunol* **180**, 1800-1807 (2008).

Table 1: Patients description

Clinical parameter	Crohn's disease n=27	Healthy controls n=23
Male/Female, n	12 / 15	15 / 8
Age at enrolment, mean ± SD, yr	45.18 (± 11.54)	60.95 (± 15.35)
Disease duration, mean ± SD, yr	9.46 (± 6.82)	-
Smoking status, yes/no/ex	10/13/4	
Crohn's disease location, n*		
L1 (ileal)	15	-
L2 (colonic)	0	-
L3 (ileocolonic)	12	-
L4 (upper disease)	0	-
Crohn's disease behavior, n*		
B1 (non-stricturing, non-penetrating)	6	-
B2 (stricturing)	16	-
B3 (penetrating)	5	-
Concomitant therapy at enrolment		
Antibiotics, n	1	
mesalamine, n	4	-
thiopurines, n	6	-
corticosteroids, n	2	-
Anti-TNF	4	-

Figure legends

Figure 1 In-vivo induced murine Th17 cells manifest different colitogenic properties. (A, B) Schematic representation of *in-vivo* induction of murine Th17 cells by aCD3 injection (A**,** aCD3) or by adoptive transfer of CD4$^+$CD25$^-$ naïve splenic CD4$^+$ T cells (B, AT1). Right-end parts of the schemes in A and B, colitogenicity evaluation of *in vivo*-generated Th17 cells by adoptive transfer of intestinal IL-17^{eGFP+} T cells into a second *Rag1$^{-/-}$* recipient (aCD3-AT2 and AT2 transfers). (C, D) Representative dot plots (C) of IL-17A and IFNγ secretion by murine LP CD4+ T cells upon aCD3 injection (upper panels, SI-derived cells) or upon adoptive transfer of naïve splenic T cells (AT1, lower panels, colon-derived cells). Right-end panels, IL-10 and IL-22 secretion by IL-17-producing T cells. (D) Frequency of IL17 and IFNg producing CD4+ T cells in the small intestine, colon and mesenteric LNs of aCD3 (white bars) and AT1 (black bars) mice. (E,F) Histological evaluation (E) and colon length (F) of *Rag1$^{-/-}$* mice untransferred (closed triangle) or 3 weeks after adoptive transfer (Open circles, AT1 mice; open triangles, aCD3AT2 mice; closed circles, AT2 mice). Scalebar, 100 µm (G,H) Colonic expression of (G) *mcp-1, il-8, cxcr3, ccl20, cxcl10* and (H) *tnf* in *Rag$^{-/-}$* mice 3 weeks after adoptive transfer of *in-vivo* induced Th17 cells (from aCD3 injection, white bars; from adoptive transfer, black bars). (I,J) Frequency of IL-17, IFNγ, IL-10 and IL-22 (I) and of IL17/IFNg (J) producing CD4$^+$ T cells in colon, small intestine and mesenteric LN of aCD3-AT2 and AT2 mice 3 weeks after transfer. (K) CD69 and α4β7 expression on colonic CD4$^+$ T cells isolated from aCD3AT2 (white bars) and AT2 mice (black bars) 3 weeks after transfer. (L) Ki-67 expression on colonic CD4+ IL-17^{eGFP+} T cells isolated from aCD3AT2 and AT2 mice. aCD3 n=6, AT1 n=15 mice; aCD3-AT2 n=11, AT2 n=14 mice analysed in 8 independent experiments. Outliers were detected with Grubb's test. Significance was

determined using unpaired two-tailed Mann-Whitney test and expressed as mean±SEM. P < 0.05 (*), P < 0.001 (***) were regarded as statistically significant.

Figure 2 *Absence of IFNγ reduces murine Th17 cells colitogenic capacity in vivo.* (A) Schematic representation of Th17 cells colitogenicity upon the repetitive adoptive transfer of IFNγ-sufficient or -deficient *in-vivo*-generated IL-17-producing CD4$^+$T cells. (B, C) Histological evaluation (B) and colon length (C) of *Rag1$^{-/-}$* mice: untransferred (closed triangle), adoptively transferred with colonic Th17 cells IFNγ-sufficient (*IFN$\gamma^{+/+}$*AT2 open circles) or deficient (*IFN$\gamma^{-/-}$*AT2 mice, closed circles). Scale bar, 100 µm (D) Frequency of cytokines (IL-17A, IL-10, IL-22) secreted by colonic CD4$^+$ T cells in *IFN$\gamma^{+/+}$*AT2 mice, open circles, or in *IFN$\gamma^{-/-}$*AT2 mice, closed circles. (E) Colonic expression of *mcp-1, il-8, ccl20, cxcl10* in IFN$\gamma^{+/+}$AT2 (white bars) or IFN$\gamma^{-/-}$AT2 (black bars) cells. (F) IF analysis of ccl20 expression in colons of IFN$\gamma^{+/+}$AT2 and IFN$\gamma^{-/-}$AT2. (G) Colonic expression of *TNF* IFN$\gamma^{+/+}$AT2 (white bars) or IFN$\gamma^{-/-}$AT2 (black bars) mice. (H) LPS levels in sera of untreated *Rag$^{-/-}$* (grey bars), IFN$\gamma^{+/+}$AT2 (white bars) or in IFN$\gamma^{-/-}$AT2 mice (black bars). (I) intestinal ZO-1 expression in IFN$\gamma^{+/+}$AT2 (left panel) or IFN$\gamma^{-/-}$AT2 (right panel). IFN$\gamma^{+/+}$ n=10, IFN$\gamma^{-/-}$ n=9 mice from 3 independent experiments. Outliers were detected with Grubb's test. Significance was determined using unpaired two-tailed Mann-Whitney test and expressed as mean±SEM. P < 0.05 (*),were regarded as statistically significant.

Figure 3. *Ileal CD4+ T cells of CD patients are enriched in IL-17$^+$IFNγ^+ T cells.* Representative dot plots (A, B**)** and cumulative statistical analysis **(**C, D**)** of IL-17A, IFNγ, TNF, IL10 and IL22 produced by ileal lamina propria CD4$^+$ T cells isolated from Chron's

disease patients (CD, n=11) and healthy donors (HD, n=9). **(E)** Representative dot plot of IL-17 produced by LP CD4^{+} T cells derived from HD (upper panel) and CD patients (lower panel) after *ex-vivo* IL-17A secretion assay **(F)** Expression levels of *IL-17a* in IL-17A^{-} (white bars) and IL-17A^{+} (black bars) ileal CD4^{+} T cells sorted upon IL-17A secretion assay of HD (n=7) and CD (n=13) LPMC. **(G)** Hierarchical clustering by average linkage of Pearson's distance of Th1-,Th2-,Th17-,Th22- and Treg-associated gene expression profile in IL-17^{-} and IL-17^{+} ileal CD4+ T cells sorted sorted upon IL-17A secretion assay of HD (white bars, n=7) and CD (black bars, n=13) LPMC. Colour intensity reflects gene expression levels. (H, I) Scatter plot (H) and (I) functional annotation clustering analysis of differentially expressed genes between IL-17A^{+} and IL-17A^{-} sorted CD4^{+} T cells from CD and control samples. Significant Annotation clusters (ES >1.3) of representative GO terms for the 211 differentially expressed genes (I) and (J) the heatmap displaying the fold changes in expression levels of selected gene subsets, in Crohn's versus the normal sample. * P ≤0.05; ** P ≤0.01 *** P ≤0.001 Mann-Whitney's unpaired two-tailed t test. Mean value ± SEM are reported.

Figure 4. *Human Th1-Th17 cells are pathogenic towards epithelial cells.* (A) Representative dot plot of double IL-17A-IFNγ secretion assay by CD-derived ileal LP CD4^{+} T cells. (B) Frequency (left panel) and total number (right panel) of Th1, Th1-17 and Th17 ileal CD4^{+} T cell clones derived from LPMCs of 6 independent treatment-naïve CD patients. (C) Representative dot plots of the cytokine profiles of Th1 (left panel), Th1-17 (middle panel) and Th17 (right panel) clones 2 weeks after cloning. (D) Multiplex analysis of IL-10, GM-CSF, TNF, IL-17A and IFNγ concentrations in the supernatants of polyclonally stimulated Th1 (left panels), Th1-17 (middle panels) and Th17 (left panels)

clones. (E) Trans-epithelial resistance (TEER) measured upon co-culture of Caco-2 cells alone (open circles) or with supernatants of unstimulated (closed circles) or polyclonally stimulated (red circles) Th1 (left panel), Th1-17 (middle panel) and Th17 (right panel) clones, or with rIL1β and rTNF (grey circles). (F) ZO-1 IF staining of Caco-2 cells 48 hours after incubation with supernatants of unstimulated (upper rows) or polyclonally stimulated (lower rows) Th1 (left panels), Th1-17 (middle panels) and Th17 (right panels) clones. Scale bar, 10 μm (G) *ccl20* expression by Caco-2 exposed 48 hours to supernatants of unstimulated (white bars) or stimulated (grey bars) Th1, Th1-17 and Th17 clones, or to rIL1β and rTNF (black bars) * P ≤0.05; *** P ≤0.001 Mann-Whitney's unpaired two-tailed t test. Mean value ± SEM are reported.

Figure 5 *Blockade of IFNγ abolishes human T cell clones pathogenicity in vitro* (A) Trans-epithelial resistance (TEER) measurement 48 hours after exposure of Caco-2 cells to supernatants of Th1 (left panel), Th1-17 (middle panel) and Th17 (right panel) clones left unstimulated (open circles), polyclonally stimulated (closed circles) or polyclonally stimulated in the presence of neutralizing anti-IFNγ (red circles) antibodies. (B) *cld2, ocln, f11r and tjp1* expression by Caco-2 exposed for 48 hours to supernatants of unstimulated (white bars) or polyclonally stimulated Th1 and Th1-17 clones in the absence (grey bars) or presence (black bars) of neutralizing anti-IFNγ antibodies. (C) ZO-1 IF staining of Caco-2 cells 48 hours after exposure to supernatants of Th1 (left panels) and Th1-17 (middle panels) clones left unstimulated (upper rows), polyclonally stimulated (middle rows) or polyclonally stimulated in the presence of neutralizing anti-IFNγ antibodies (lower rows). * P ≤0.05; *** P ≤0.001 Mann-Whitney's unpaired two tailed t test. Mean value ± SEM are reported.

Figure 1

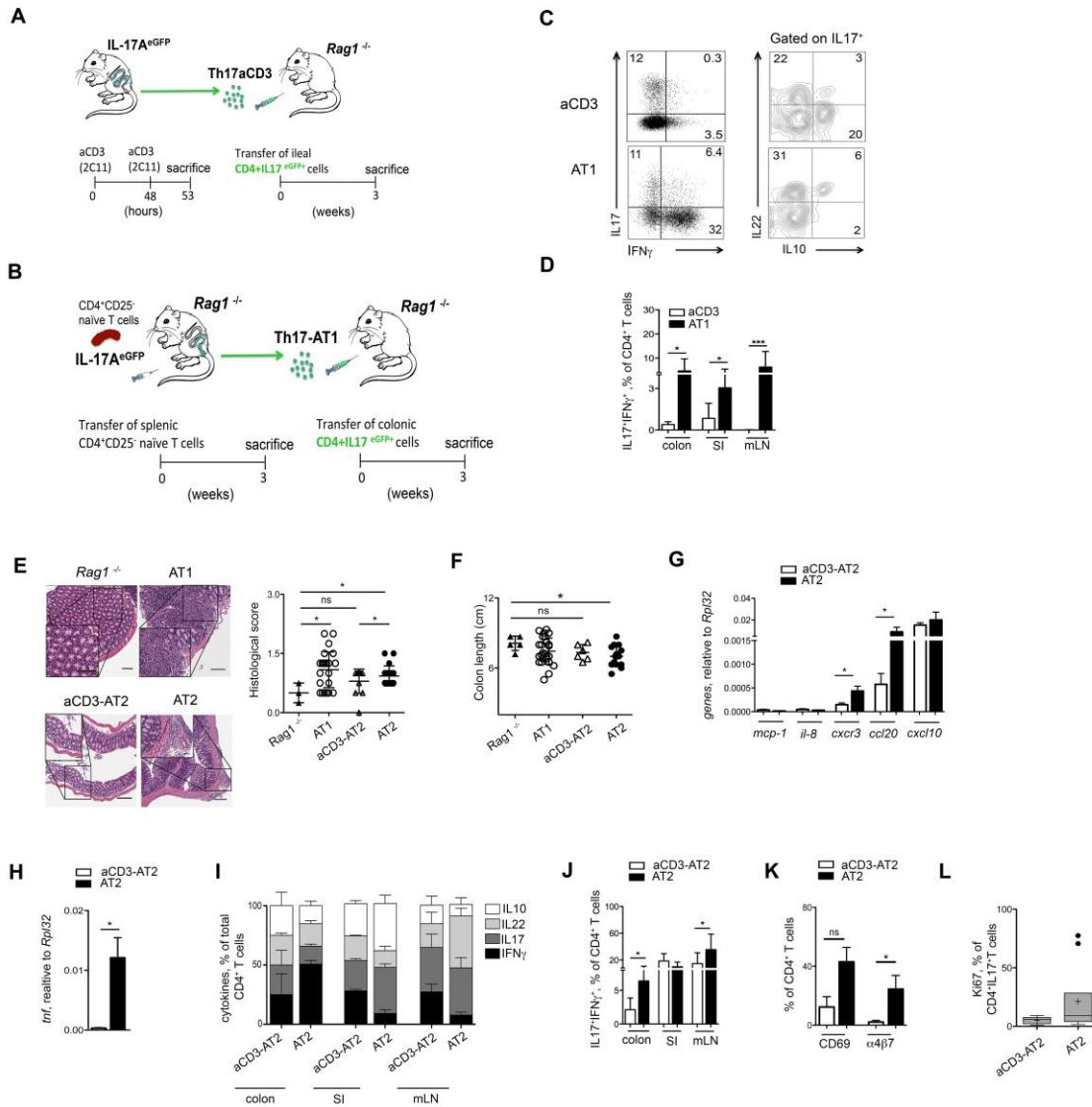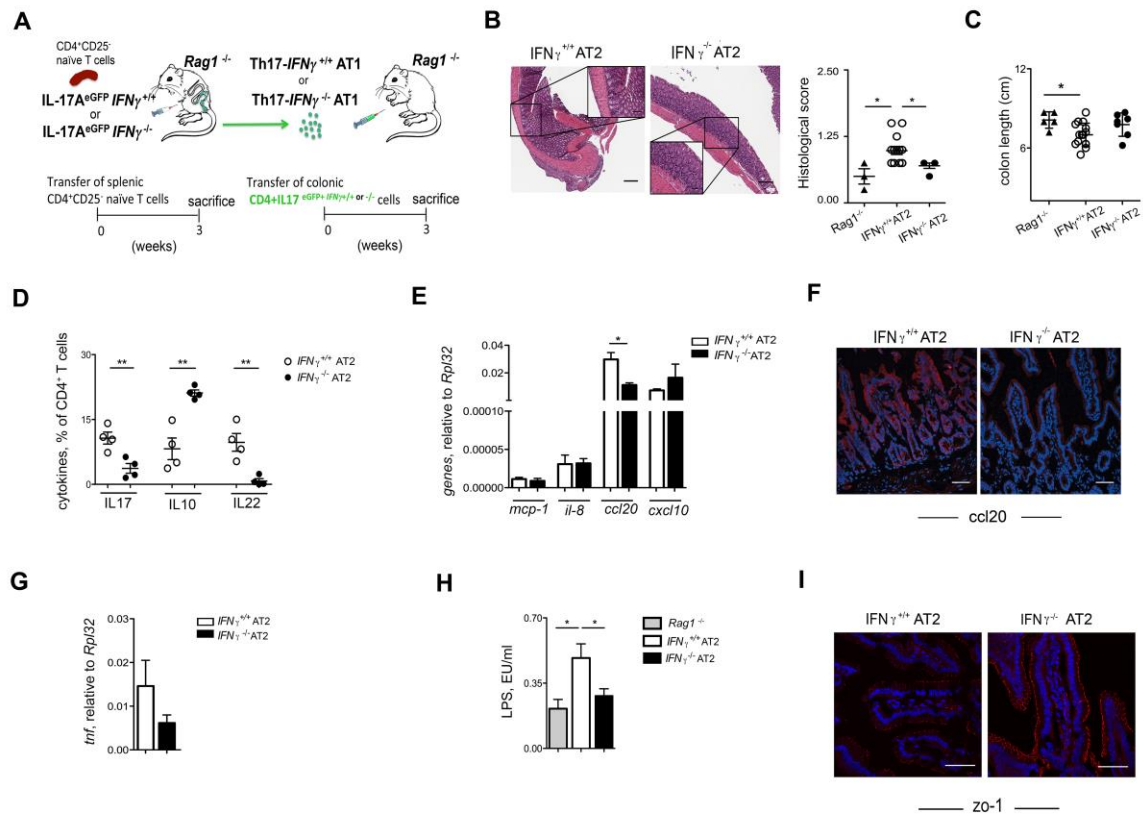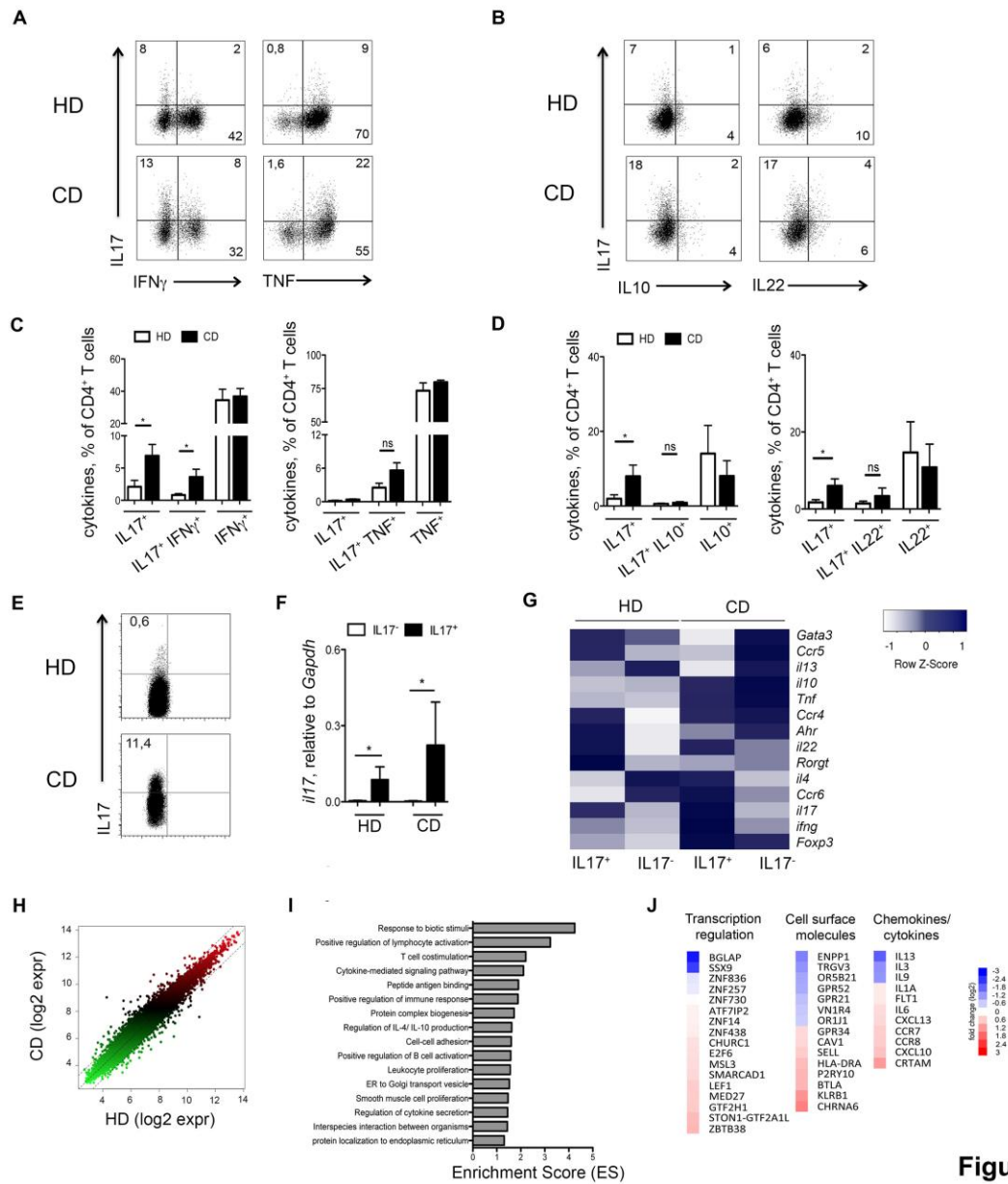**Figure 2.**

Figure 3.

Figure 3

Figure 4.

Figure 4

Figure 5.

Figure 5